Scientific paper

Three-Dimensional Cyclic Behavior Simulation of RC Columns under Combined Flexural Moment and Torsion Coupled with Axial and Shear Forces

Satoshi Tsuchiya[1], Koichi Maekawa[2] and Kazuhiko Kawashima[3]

Received 20 December 2006, accepted 4 August 2007

Abstract

Full three-dimensional nonlinear finite element analysis based on the path-dependent non-orthogonal multi-directional crack model is applied to RC columns subjected to combined cyclic flexure/shear and torsion. This loading causes non-orthogonal crack-to-crack mechanistic interactions accompanying opening/closure and shear slip along crack planes. The analytical results show that the proposed methodology is able to simulate the highly nonlinear behavior of RC columns under cyclic loading, including not only load-carrying capacity but also complex restoring force characteristics and post-peak softening after peak strength. Sensitivity analysis is also carried out to examine the effectiveness of the transverse reinforcement, which simultaneously resists both transverse shear and torque moment. The current design procedure for determining the necessary and sufficient amount of web reinforcement is reviewed and the necessity of performance assessment is raised.

1. Introduction

The past two decades have seen investigations of single-crack kinematics and interactions among non-orthogonally intersecting cracks, leading to space-averaged reinforced concrete (RC) path-dependent constitutive models (Collins and Vecchio 1982, Maekawa *et al*. 2003). As a result of this work, full three-dimensional nonlinear structural analysis is becoming a practical method of behavioral simulation for structural concrete. Since no degeneration of the stress/strain field takes place, in contrast with the in-plane theorem, computational solutions are self-consistent and highly applicable to analysis domains with geometry and boundary conditions of any complexity. Although computational efficiency tends to be lower than for analysis based on in-plane frames or layered shells when the FEM nodal degree of freedom exceeds approximately 10,000, high-speed sparse matrix solvers and parallel computing currently enable us to run nonlinear simulations within reasonable time (Maekawa *et al*. 2006). Furthermore, the reliability of the analysis has been greatly improved through multi-faceted verifications. Currently, full three-dimensional nonlinear analysis is being used for the assessment of structural performance in design as well as in the maintenance of existing infrastructures.

[1]Representative Director, COMS Engineering Corporation, Japan.
E-mail:satoshi@comse.co.jp
[2]Professor, Department of Civil Engineering, University of Tokyo, Japan.
[3]Professor, Department of Civil Engineering, Tokyo Institute of Technology, Japan.

RC columns under torsion are a typical 3D problem of practical engineering interest. In general, pure torsion rarely arises in structural concrete. Rather, it is normally tied in with simultaneous flexure and shear. Since so-called ductility design, in which high plasticity is assumed, has reached mainstream practice, several experimental studies have been conducted to examine the interaction between flexural shear and torsion (Nagataki *et al*. 1988, Collins *et al*. 1991). In these investigations, attention focused on member capacity and there was less discussion of the translational ductility of seismic resistant members under coupled torsion and flexural shear. To ensure safety, the general practice is to provide transverse reinforcement first based on flexural shear design and then simply add the requisite reinforcement corresponding to the torsion. This does not take into account the nonlinear interaction between translational restoring force and torsion. Consequently, this conservative approach tends to result in an excessive amount of transverse reinforcement, sometimes causing great difficulty in concrete placement and rising costs. Recently, a number of loading experiments have been carried out to investigate this issue by Yukawa *et al*. (1999), Hsu *et al*. (2000), and Otsuka *et al*. (2005). Tirasit and Kawashima (2005, 2006, 2007) reported a series of experiments on RC columns subjected to a full combination of axial force, flexural shear and torsion.

As a verification of the constitutive modeling based on the smeared multi-directional cracks (Maekawa *et al*. 2003), the authors reported on the full three-dimensional nonlinear analysis (Tsuchiya *et al*. 2002) of RC solid columns conducted by Matsuzaki *et al*. (2002). In this case, the mechanical parameters were permanent eccentric axial force, reversed cyclic flexural shear and torsion. It was verified that the simulation was able to approximately evaluate the restoring force characteristics with interaction among eccentric axial force, flexure/shear and torsion. However, the post-peak residual forces were excluded from the scope and the number of verification cases was also limited. Since then, much progress in the post-peak time dependency and fracture analysis of structural concrete has been achieved (El-Kashif *et al*. 2004a, b, Maekawa *et al*. 2004). Thus, the authors' first aim in this study is to discuss the applicability of the most recent time-dependent full three-dimensional nonlinear analysis in simulating recent systematic experiments by Tirasit and Kawashima (2005, 2006, 2007). This experimental study clearly presents 3D structural behavior of great complexity even in the post-peak region, and delivers useful information for the practical design of bridge columns. Thus, the authors have selected this series of experiments as suggestive work. The second aim of the study is to carry out sensitivity analysis to allow a discussion of rational design of transverse reinforcement that resists both transverse shear and torsion around the member axis.

2. Experiment with RC columns subjected to full combination of section forces

This section outlines the series of experiments carried out by Tirasit and Kawashima (2005, 2006, 2007), based on which the numerical analysis and the constitutive laws of path- and time-dependency are to be verified. The structural dimensioning and detailing of the specimens are shown in **Fig. 1**. The specimens were designed in accordance with the Japanese highway bridge code (Japan Road Association 1996). The cross section is 400-mm square and sufficient tie reinforcement is provided. The height of the loading point is 1.35 m from the bottom of the column. After fixing the specimen footings using pre-stressing bars in the vertical direction, a constant axial force (0 or 160 kN) was applied using a hydraulic actuator. Flexural shear and torsion were simultaneously applied using twin horizontal actuators, as shown in **Fig. 2**. Twist and translational displacement were applied interdependently in such a manner that the index denoted by r was:

$$r = \theta/\Delta = constant \qquad (1)$$

where θ = column rotation (radian), Δ = lateral drift (%).

For reference, **Fig. 3** describes the loading history of flexural shear and torsion in the previous study by Matsuzaki *et al*. (2002). For this specific loading, full three-dimensional analysis has already been carried out, yielding a reasonable simulation (Tsuchiya *et al*. 2002). It should be noted that the loading path specified by Eq. (1) greatly differs from previous experimental studies and is thought to reflect real loading states more closely. As shown in **Table 1**, seven loading experiments were conducted (P1 to P7) for the specimens of the same structural dimensions under different combinations of translational displacement and twist angle with and

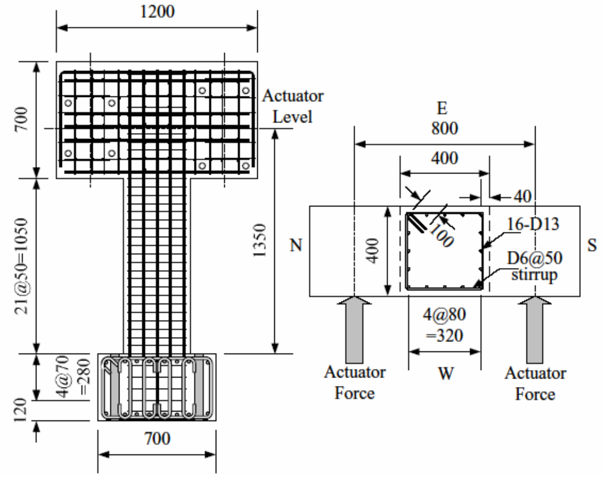

Fig. 1 Structural dimensions of specimen (Tirasit *et al*. 2005, 2006, 2007).

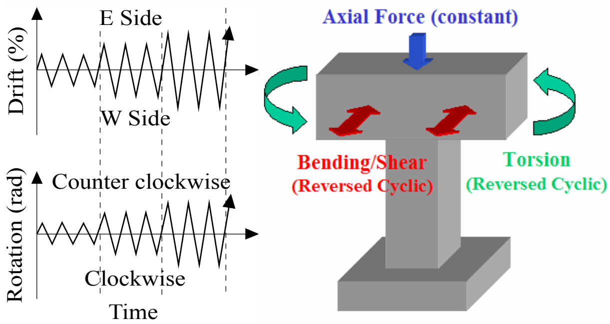

Fig. 2 Loading using two horizontal actuators (Tirasit *et al*. 2005, 2006, 2007).

Table 1 Loading cases and material strengths (Tirasit *et al*. 2005, 2006, 2007).

Column No.	Loading Scheme	r by Eq. (1)	Concrete f'_c (MPa)	Steel f_y (MPa)
P1	M+P	0	28.6	D13: 353.7
P2	T	∞	28.3	
P3	T+P	∞	28.4	
P4	T+M+P	0.5	32.2	
P5	T+M+P	1.0	28.4	D6: 328.0
P6	T+M+P	2.0	32.8	
P7	T+M+P	4.0	33.1	

 # T: Cyclic torsion, M: Cyclic uni-axial flexure, P: Constant axial compressive force (160 kN)

without axial forces. Three-cycles of load hysteresis were applied at each displacement. The material properties are also given in **Table 1**.

Figures 4 to **10** show the experimental results, consisting of relationships between the horizontal load and corresponding displacement as well as the torque-twist relation measured at the loading point in each case.

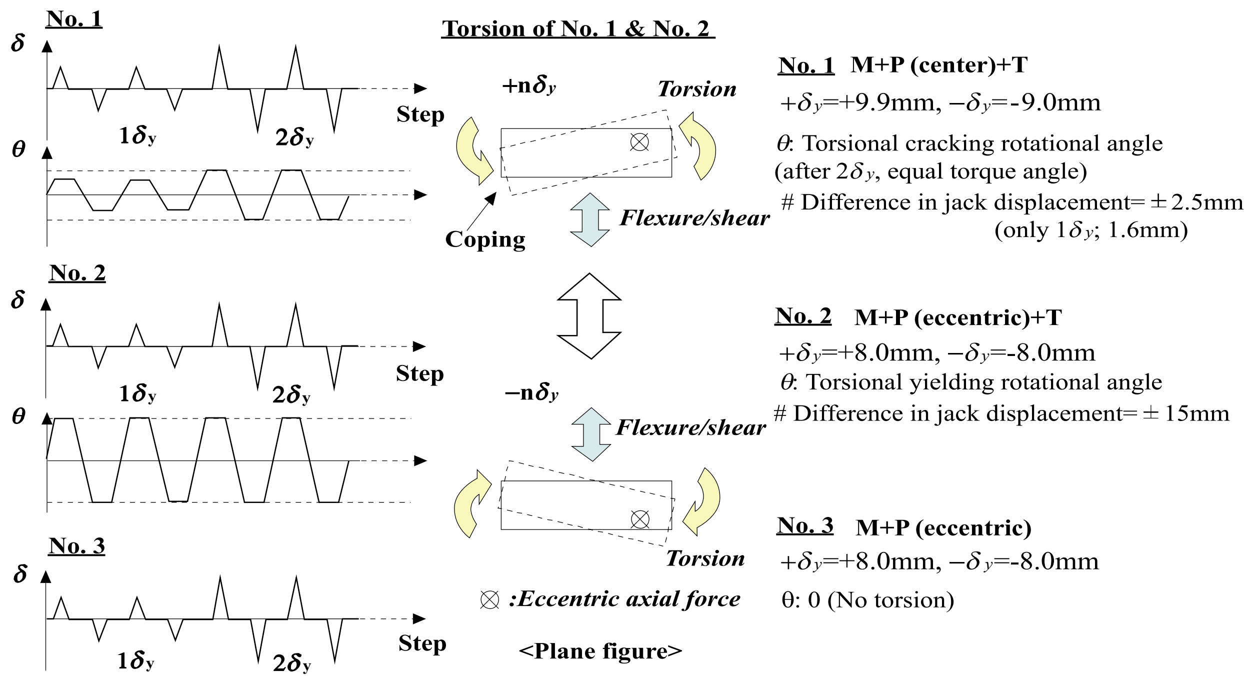

Fig. 3 Loading using two horizontal actuators (Matsuzaki *et al*. 2002, Tsuchiya *et al*. 2002).

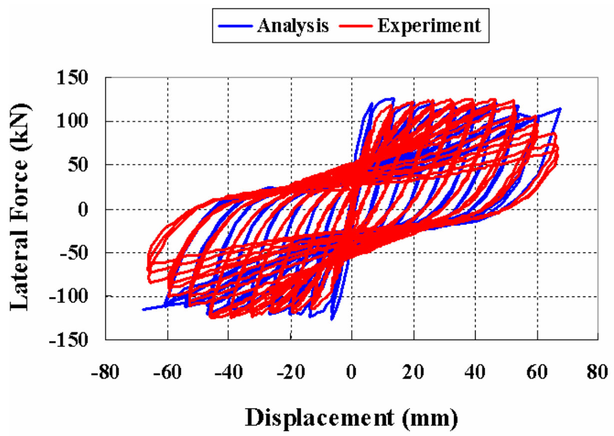

Fig. 4 Experimental and analytical results for P1 (no torsion).

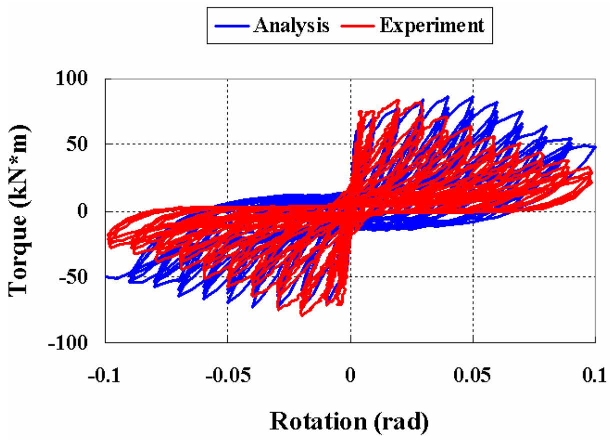

Fig. 6 Experimental and analytical results for P3 (torsion + axial force).

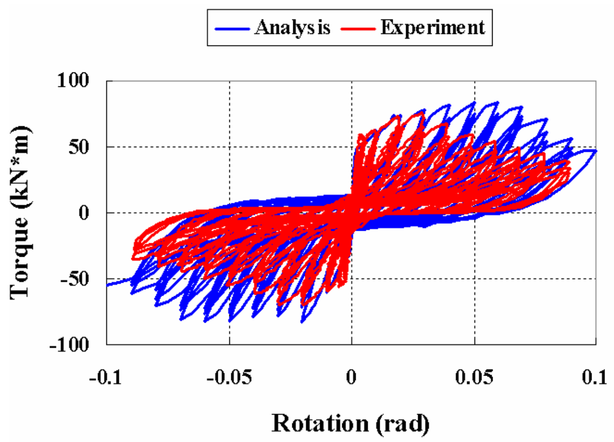

Fig. 5 Experimental and analytical results for P2 (pure torsion).

These results are purely extracted structural responses by carefully considering some influences of loading devices (Nagata *et al*. 2004, 2005). Namely, the geometrical nonlinear P-Δ effect, as caused by the vertical actuator, is subtracted and the actually applied horizontal forces and torque moments are shown in the figures. It is clearly identified that flexural load-carrying capacity and translational ductility gradually decline as the induced torque increases. This series of loading patterns is of practical use in the verification of computational simulations as well as in the investigation of design criteria.

Looking at the experimental results, specimen P1 (axial force and cyclic flexure/shear only) exhibited eventual spalling of the cover concrete and buckling of the main reinforcing bars at about 200 mm height from

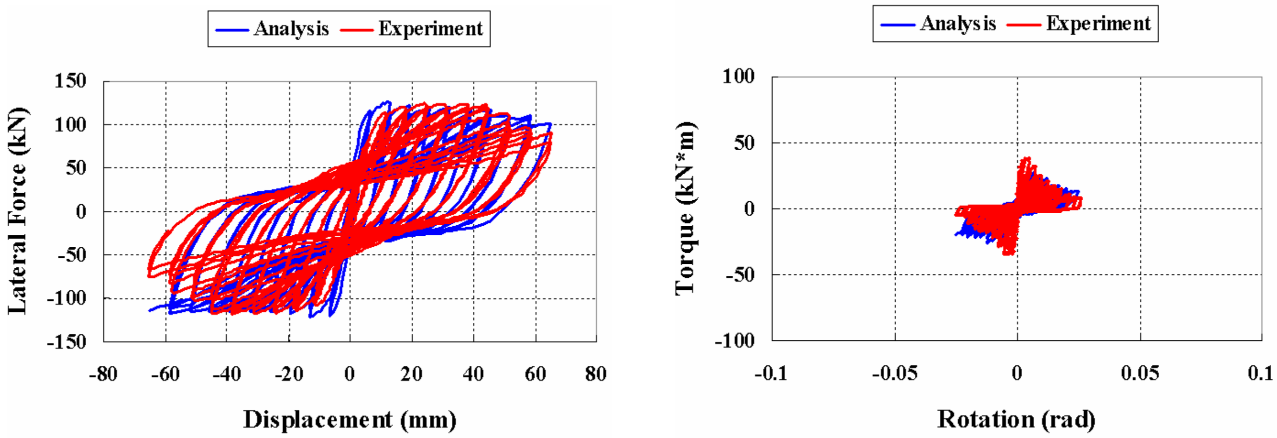

(a) Lateral force and displacement relationship (b) Torque and rotation relationship

Fig. 7 Experimental and analytical results for P4 (full combination).

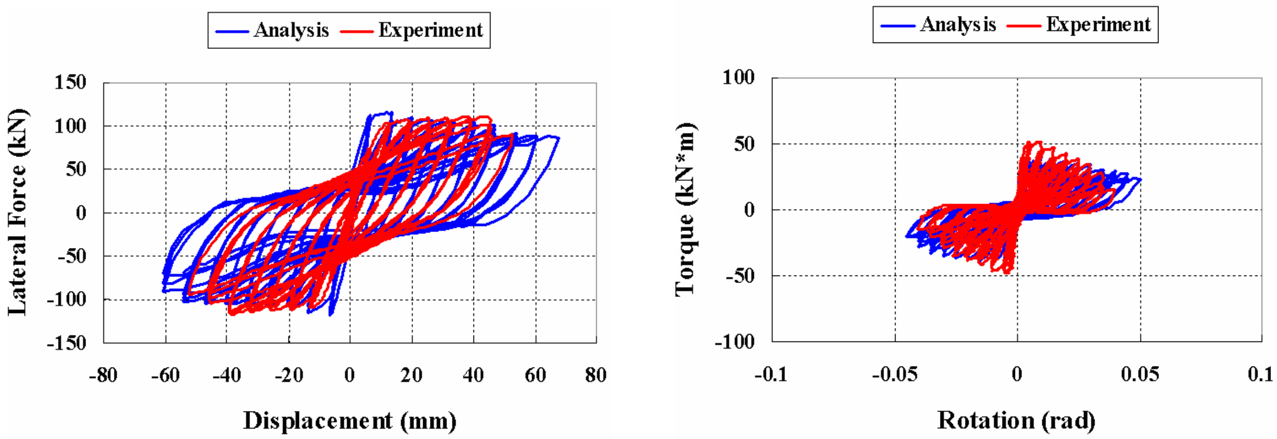

(a) Lateral force and displacement relationship (b) Torque and rotation relationship

Fig. 8 Experimental and analytical results for P5 (full combination).

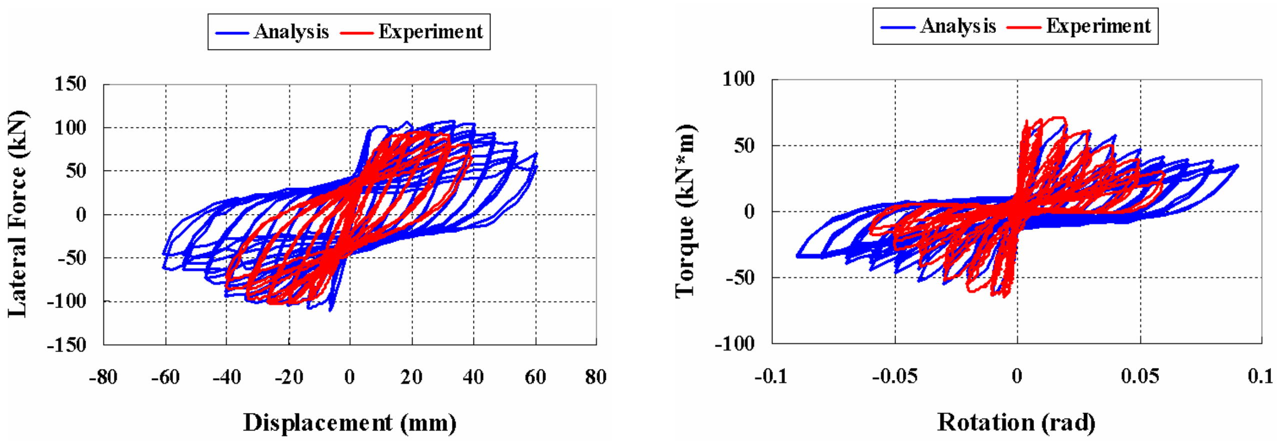

(a) Lateral force and displacement relationship (b) Torque and rotation relationship

Fig. 9 Experimental and analytical results for P6 (full combination).

the column base, resulting in a decrease in load-carrying capacity. In specimens P2 and P3 (cyclic torsion applied), dispersed inclined cracks appeared on all surfaces of the columns, predominantly around mid height. The cover concrete eventually spalled out and the main reinforcing bars buckled outward slightly. In these two

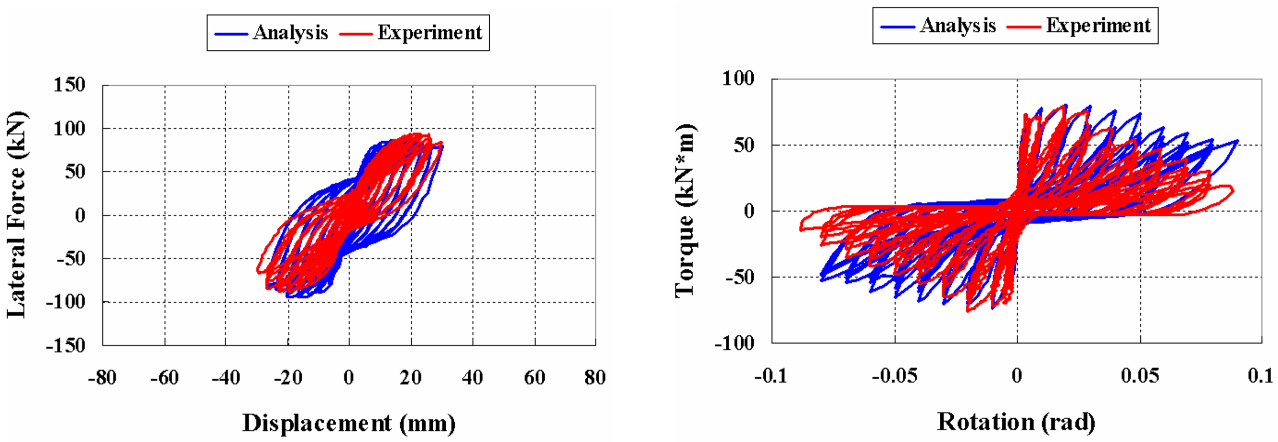

(a) Lateral force and displacement relationship (b) Torque and rotation relationship

Fig. 10 Experimental and analytical results for P7 (full combination).

cases, torque strength and initial stiffness are larger in specimen P3 (with axial force) than in P2 (without axial force) and the inclination of the diagonal cracks is also greater in the P3 case. With specimens P4 to P7 (full combination of axial force, shear, flexure and cyclic torsion), the levels of damage lie between those of P1 and P3 depending on the magnitude of twist around the member axis. Specimens P4 to P7 are suitable for verification of the path-dependent multi-directional smeared fixed crack model because non-orthogonal cracks (diagonal cracks caused by torsion and shear, and horizontal cracks by flexure) develop in more than three non-orthogonal directions and the primary crack direction varies from time to time. All important data related to these experiments have been made available to the public in digital form through the Internet by Kawashima (2006).

3. Details of full three-dimensional finite element nonlinear analysis and modeling

The full three-dimensional nonlinear analysis used in this paper is formed by extending the in-plane RC constitutive model to cover 3D stress states (Maekawa *et al.* 2003). In the plane stress field, the multi-directional smeared fixed crack method is adopted with path-dependent constitutive laws for the concrete solid and crack planes (Okamura *et al.* 1991). Non-orthogonal crack-to-crack interaction can be treated by the active crack method under cyclic stresses and four-directional cracking can be represented within a control volume for which the space-averaged stress-strain relation is defined. By adopting opening/closure kinematics, slip along crack planes and their interactions among cracks in four non-orthogonal directions, the model is able to identify the stress-carrying mechanics of cracked RC domains under arbitrary loading paths. **Figure 11** shows the simplified decomposition of the three-dimensional stress field with crack damage reduced to the two-dimensional sub-mirror spaces on which the in-plane constitutive model is applied. Further details of these analytical and full-three dimensional constitutive models of cracked concrete are discussed in the references (Maekawa *et al.* 2003, 2006). As noted in the previous section, model accuracy especially in softening regions after the peak capacity is currently enhanced by upgrading the constitutive models of concrete compression in terms of time-dependency (El-Kashif *et al.* 2004a, b, Maekawa *et al.* 2004). The ductility of RC columns subjected to flexure and torsion is also affected by local spalling of the cover concrete and buckling-like transverse deformation of reinforcing bars. Thus, spatially averaged models for both concrete spalling and post-buckling of reinforcing bars (Dhakal *et al.* 2002a, b) are introduced into the three-dimensional analysis.

Isoparametric elements consisting of 20 nodes are used to promote higher-order interpolation of strain fields and to reduce the number of elements while maintaining reasonable accuracy. Concrete elements close to or around embedded reinforcement are expected to have dispersed crack assemblies inside them due to bond stress transfer. Here, a group of cracks is represented mechanically as a whole by post-cracking tension-stiffness modeling defined for the elements concerned (RC zone). In contrast, concrete elements located far from the reinforcement may contain only a single crack due to localization and the strain-softening modeling is applied (Plain zone). A simple way to identify these RC and plain zones was proposed by An *et al.* (1998) and a finite element discretization consistent with this was defined as shown in **Fig. 12**. The width of the RC zone is simply defined as two times the size of the cover concrete. This RC zoning-based discretization of analysis domains generally enables reasonable accuracy with a comparatively small number of finite elements and the mesh size sensitivity to the analytical results can be significantly decreased to a negligibly

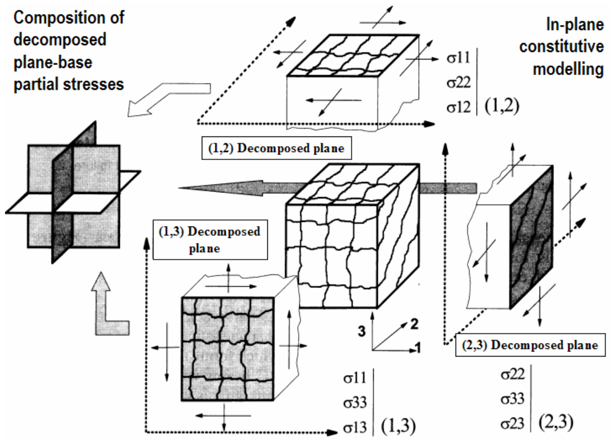

Fig. 11 Composition of sub-mirror spaces in three dimensions (Maekawa *et al*. 2003).

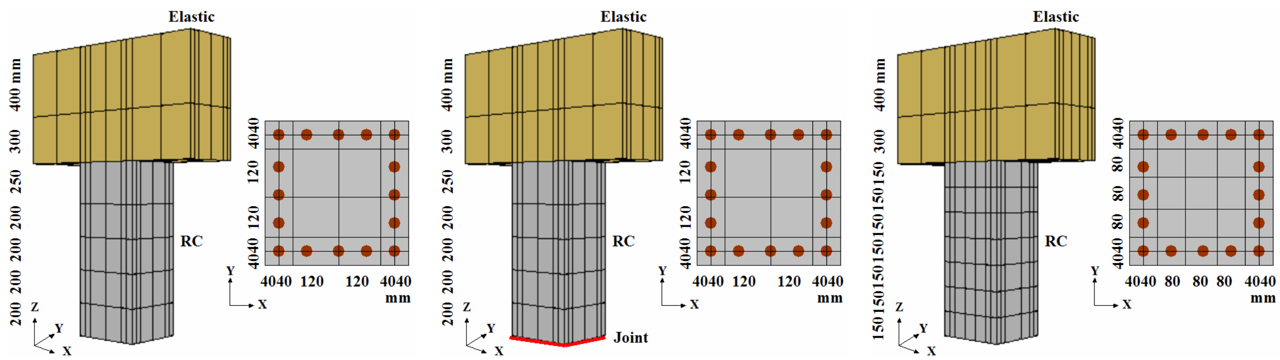

(a) Standard mesh (b) Standard mesh + Joint elements (c) Fine mesh

Fig. 12 Mesh division.

small level (An *et al*. 1998). In order to check the solution for convergence, a finer mesh solution was compared with that of the standard one (**Figure 12**) and no substantial difference was detected.

Experimental measurements have demonstrated that the local effect of pull-out of reinforcing bars from the footing is not significant provided that the ratio of reinforcing bar size to specimen cross-section is similar to that of real columns (Kosaka *et al*. 1997). In order to check this ratio, which is thought to be have low sensitivity, the authors first analyzed some cases with joint interface elements placed between the main body of the column and the footing, as shown in **Fig. 12** (Okamura *et al*. 1991, Maekawa *et al*. 2003). Since no substantial difference was found in analyses, subsequent computations were carried out without the joint interface elements.

For defining material strength and characteristics in computation, the same values in **Table 1** are used without any re-calibrations. Elastic elements are arranged at loading points to avoid local bearing failure of the concrete. The footing is not modeled, but the displacement of all bottom nodes is fixed. In the analysis, the experimentally obtained displacement at the twin horizontal jacks is imposed under the applied axial force. No failure criteria are defined in advance, which allows the simulations to trace the entire behaviors until the end of the experiments. **Table 2** outlines the analytical cases.

Table 2 Analytical cases.

Column No.	Standard Mesh			With Joint Elements	Fine Mesh
		Sensitivity on f_y	Sensitivity on tie reinf.		
P1	○	---	$0.5*A_w$	---	---
P2	○	---	---	---	---
P3	○	---	$0.5*A_w$	---	---
P4	○	---	---	---	---
P5	○	$0.9*f_y$	$0.5*A_w$	○	○
P6	○	---	---	---	---
P7	○	$1.1*f_y$	$0.5*A_w$	---	---

 # f_y: Tensile yield strength of steel, A_w: Area of shear reinforcement

4. Analytical results and comparison

Analytically obtained horizontal load-displacement and torque-twist angle relationships at the loading point are shown in **Figs. 4** to **10** superimposed over the experimental results. The loading rate in the analysis is exactly set in accordance with that of the experiments. In general, similar flexural and torsional responses are demonstrated in analysis and experiment, although some minor deviations remain. The nonlinear FE analysis of pure torsion cases leads to somewhat overestimated torque just after maximum torsion capacity. This may be attributed to the early spalling of cover concrete in the experiment under torsion as compared with the analysis. This effect becomes significant especially when the member size is small. However, the simulation gives reasonable predictions of flexural load-carrying capacity and ductility decay induced by cyclic torque moment. In other words, torque capacity and torsional ductility are fairly well simulated as decreasing with increasing cyclic flexural shear. The analysis can approximately outline this cross-effect of torsion and flexural shear over the post-peak region.

In particular, there was no sharp decrease in flexural load-carrying capacity even after torsional capacity deterioration in the experiments (P5 around 4-5 δ_y, for example), and this is well predicted analytically. This correlation may imply that the intersection of torsion-shear diagonal cracks and transverse bending cracks is adequately embodied in the analysis. In addition, the analysis also reproduces the stiffness degeneration caused by repetitive loading in the post-peak region. In the computation, this is attributed to the high-rate plasticity and fracturing of post-peak concrete being formulated as per El-Kashif *et al*. (2004a, b) and Maekawa *et al*. (2004).

The analytical results for P5 with the finer mesh are shown in **Fig. 13**. There is little difference between these results and the results obtained with the standard mesh (**Fig. 8**). The analytical results for P5 with joint interface elements attached to consider pullout of the reinforcing bars from the footing are shown in **Fig. 14**. This detailed consideration of steel pullout improves analytical accuracy in terms of initial stiffness but there

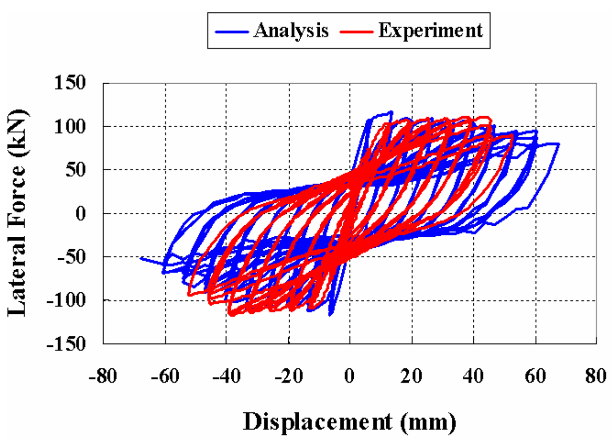

(a) Lateral force and displacement relationship

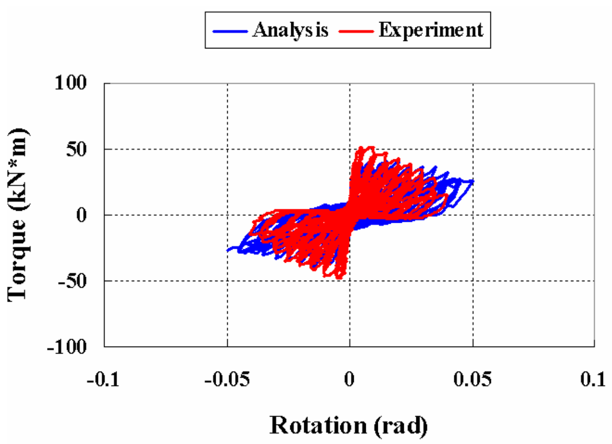

(b) Torque and rotation relationship

Fig. 13 Experimental and analytical results for P5 using fine mesh.

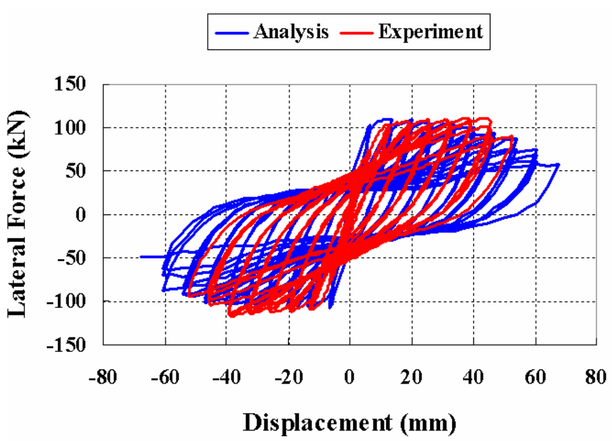

(a) Lateral force and displacement relationship

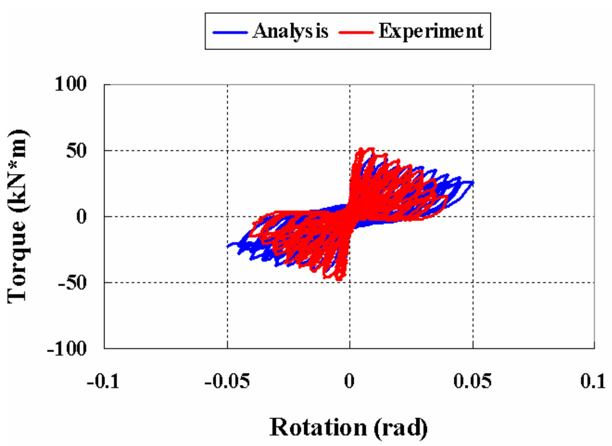

(b) Torque and rotation relationship

Fig. 14 Experimental and analytical results for P5 with joint elements introduced.

is no significant difference in the large deformational behavioral response, as described in the previous section.

Figure 15 shows the deformational modes for all cases with the standard mesh. Deformation is magnified five times for clarity. These snapshots are drawn at the first loop of the seventh cycle ($7\delta_y$ or $7\theta_y$). Combined deformation arising from flexure and torsion is clearly captured. **Figure 16** illustrates the maximum principle strain corresponding to each case in **Fig. 15** as shading contours. The highly shaded areas are concentrated near the base of the column when only flexural shear is applied (P1), while the zone of greater strain moves up to column mid-height as the magnitude of torsion increases. Regarding steel stress, the main reinforcing bars chiefly yield under flexural action and the lateral ties under the torsional moment and shear force. In this numerical analysis, a multi-frontal direct linear sparse matrix solution (Schenk *et al*. 2004) was applied with parallel computing using twin CPU cores. A few hours were required to calculate about 1,500 incremental loading steps with 300 finite elements using a standard PC. It should be noted that computation time is not very long compared with time for pre- and post-processing, even during a full three-dimensional solution run with large degrees of freedom.

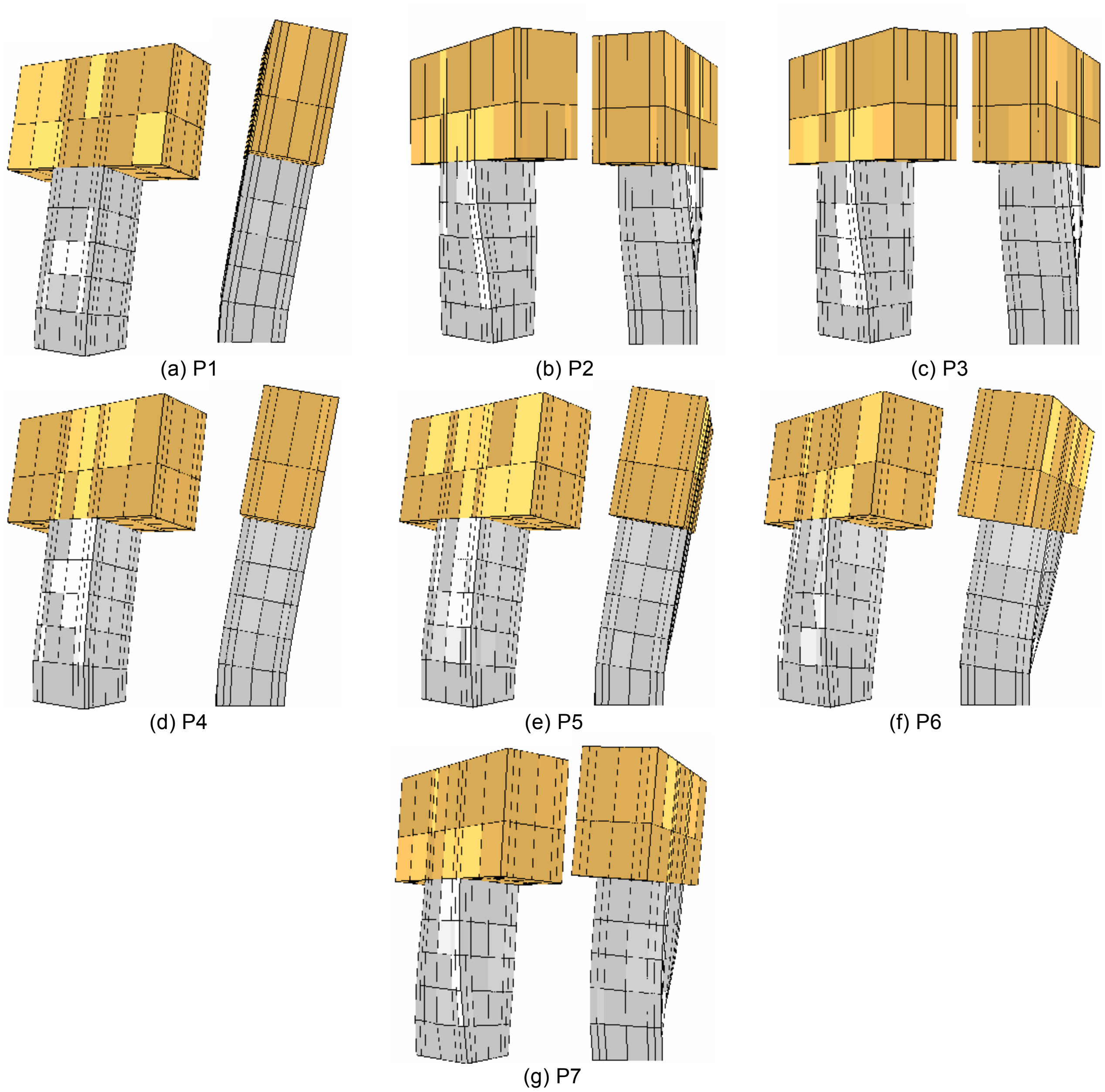
(a) P1 (b) P2 (c) P3 (d) P4 (e) P5 (f) P6 (g) P7

Fig. 15 Deformation map.

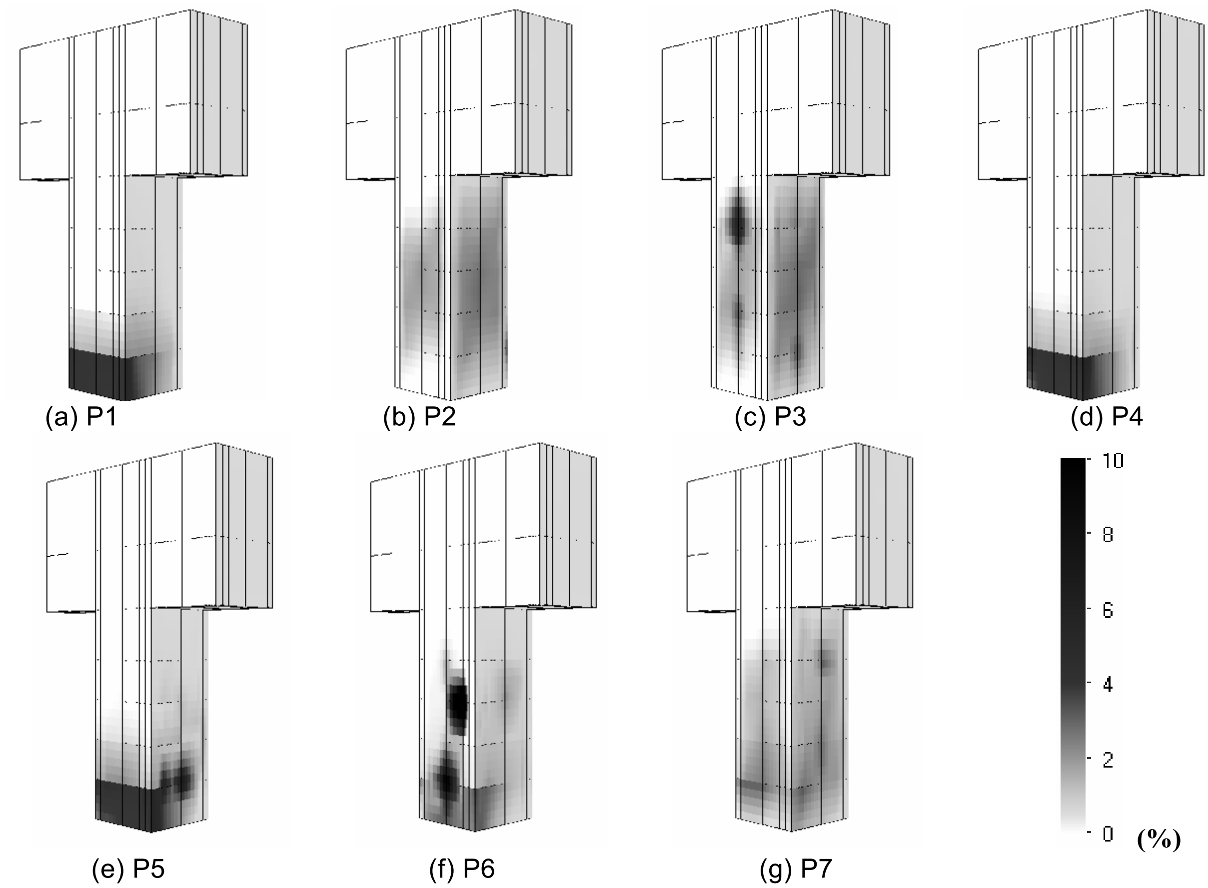

Fig. 16 Maximum principle strain contour.

5. Numerical structural performance assessment

Having confirmed the reliability of the full three-dimensional analysis, it may be productive to carry out sensitivity analysis on the yield strength of the main reinforcement and the quantity of lateral ties. In actual practice, a large amount of transverse reinforcement tends to be used, because the required amount is calculated according to the torque moment, which derives from the initial constant stiffness. But in reality, as discussed in the previous section, torsion stiffness is much reduced as the result of a crossover effect associated with translational displacement, as discussed in Chapter 4. The authors therefore examine how the amount of transverse reinforcement can be reduced while maintaining the original seismic performance.

Figure 17 and **Figure 18** show the predicted responses with regard to yield strength of the main reinforcement. The yield strength is adjusted to 0.9 times the original value for P5 and to 1.1 times for P7, respectively. The sensitivity study shows that flexural shear response follows traditional bending theory; that is, horizontal load is almost proportional to yield strength while the torsional response is not affected at all even after the point of primary plasticity. These results confirm the explanation given in the previous section for steel stress and represent the influence of main reinforcement yield strength on the overall nonlinear response.

Next, sensitivity analysis on the lateral ties is considered. Transverse reinforcement influences construction efficiency and concreting work greatly. Excessive lateral ties may sometimes cause initial defects due to imperfect consolidation of fresh concrete. This means that a necessary and sufficient amount of lateral ties is essential for consistent design that satisfies manifold performances.

The ratio of tie reinforcement is reduced to 50% of the original value in P1, P3, P5 and P7. Corresponding analytical results are shown in **Fig. 19** to **Fig. 22**. According to the JSCE concrete standard specifications (JSCE 2002), shear capacity still exceeds that of flexural yielding in all cases. It is confirmed that torsional strength declines remarkably in the case of pure torsion as well as when flexural shear and torsion are coupled, while flexural capacity is less affected and only ductility falls slightly for both pure flexural shear and combined flexural shear and torsion. These results may suggest that the design method in general, that is to say a simple

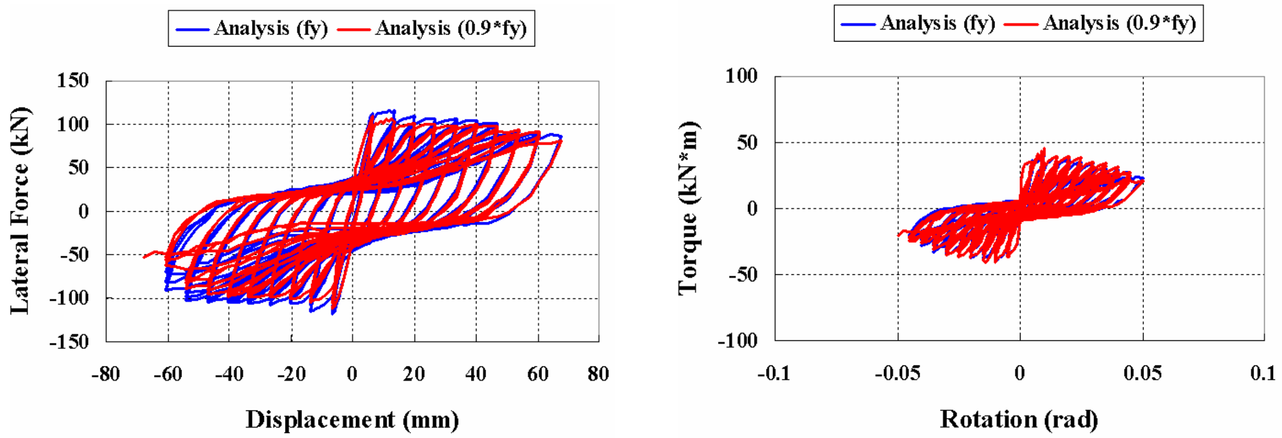

(a) Lateral force and displacement relationship

(b) Torque and rotation relationship

Fig. 17 Sensitivity analysis for P5 on yield strength of main reinforcement.

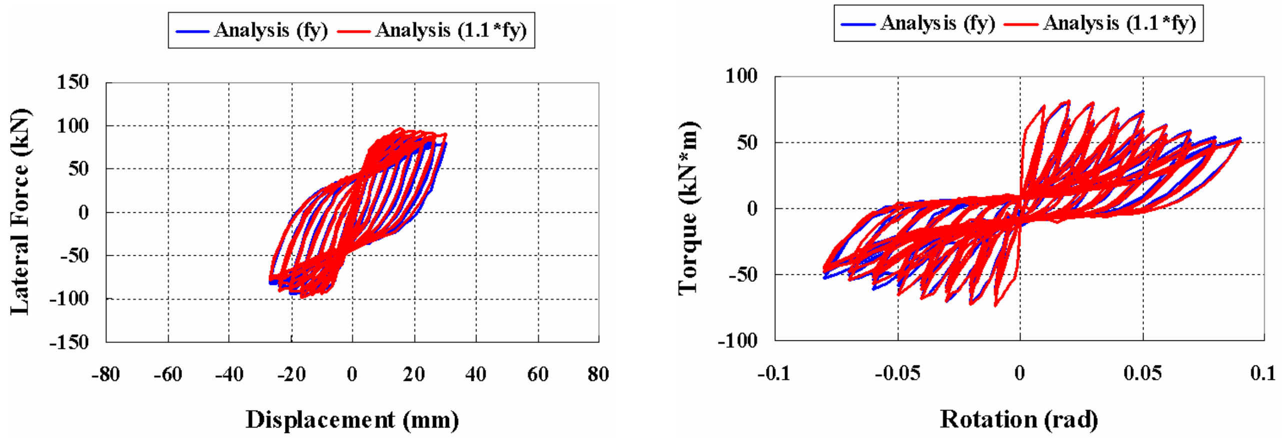

(a) Lateral force and displacement relationship

(b) Torque and rotation relationship

Fig. 18 Sensitivity analysis for P7 on yield strength of main reinforcement.

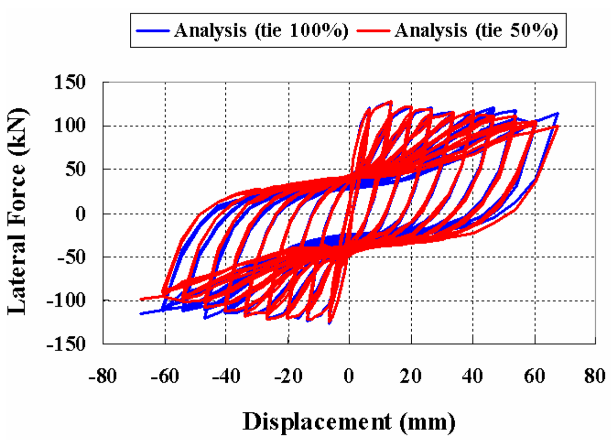

Fig. 19 Sensitivity analysis for P1 on tie reinforcement.

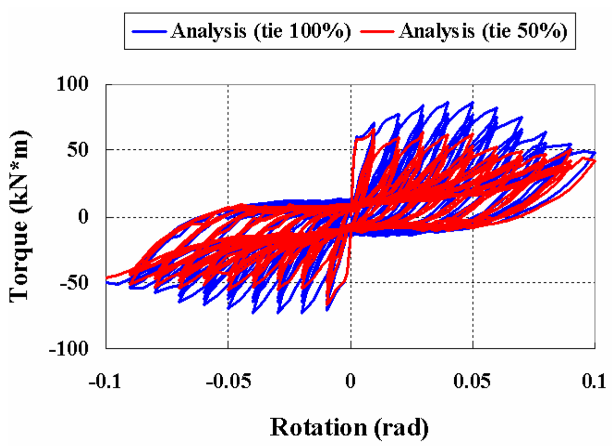

Fig. 20 Sensitivity analysis for P3 on tie reinforcement.

summation of the requisite amounts required for flexural shear and for torsion, may result in over-reinforced members with respect to shear and torsion. Ideally, this excessive quantity of reinforcing ties arrived at by initial design should be reduced to a more reasonable level. Here, a computational assessment is essential to assure performance. This procedure can be expected to facilitate bar arrangements and concrete casting and therefore improve the quality of the structure as a whole.

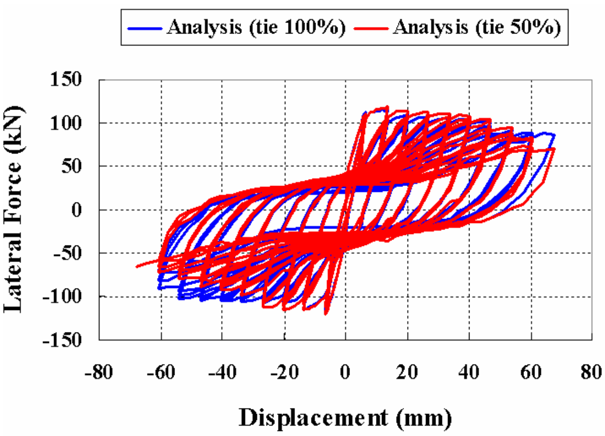

(a) Lateral force and displacement relationship

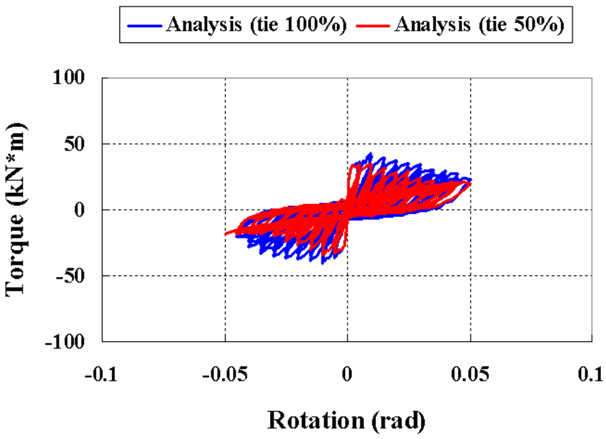

(b) Torque and rotation relationship

Fig. 21 Sensitivity analysis for P5 on tie reinforcement.

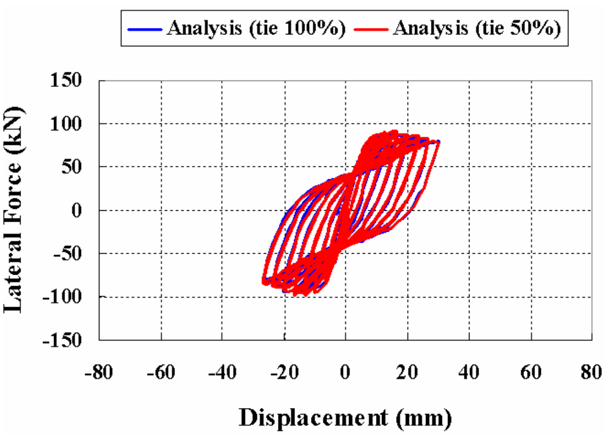

(a) Lateral force and displacement relationship

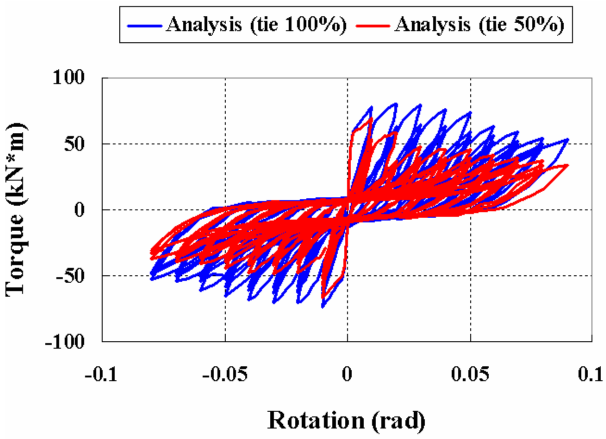

(b) Torque and rotation relationship

Fig. 22 Sensitivity analysis for P7 on tie reinforcement.

6. Conclusions

Full three-dimensional nonlinear finite element analysis based on the path-dependent non-orthogonal multi-directional crack model was applied to RC columns subjected to combined cyclic flexure/shear and torsion. The analytical results showed that the proposed methodology can simulate highly nonlinear behavior of RC columns under cyclic loading, including not only load-carrying capacity but also the complex restoring force characteristics and post-peak softening after peak strength. The analytical method is able to trace non-orthogonal crack-to-crack mechanistic interactions accompanying opening/closure and shear slip along crack planes in more than three directions. Two additional cases of sensitivity analysis were considered, one for mesh division and another for local behavior at the column base joint, but these factors was found to have only a slight influence.

Enhancement of analytical accuracy for flexure response in the post-peak region has already been achieved by taking into account large local deformation of the reinforcing bars due to buckling. On the other hand, it is well known that cover concrete spalling easily occurs under torsion. That said, it is most likely that the swelling effect of reinforcing bars under torsion differs from that of reinforcing bars subjected to flexure/shear only. These are challenges for the future that will increase accuracy.

Sensitivity analysis on the yield strength of the main reinforcement and the quantity of lateral ties was also carried out. It was found that changes in the yield strength of the main reinforcement affect flexure/shear response almost proportionally, while the torsional response is little affected for the column members dealt with in this study. It was also clarified that ductility decreases slightly in flexure/shear response, while torsional strength falls significantly when the reinforcement ratio of lateral ties is reduced by 50%. This result suggests that the general practice method, in which the quantity of transverse ties is obtained as the simple summation of the requirements for flexural shear and torsion, results in over-reinforced members with respect to shear and torsion.

The results of this study suggest that the likelihood of full three-dimensional nonlinear analysis without D.O.F. degeneration finding application in business practice is improved. It may be possible to use this method as a verification tool for 3D problems involving RC structures/members. It may also be possible to rationalize structural dimensions or bar arrangements based on a quantitative evaluation from the viewpoint of structural performance assessment. In addition, it is a great advantage that full three-dimensional nonlinear analysis does not require sophisticated engineering judgment despite heavy work on pre- and post-processing, for this allows reproduction of structural response as it is under any conditions. On the other hand, three-dimensional frame analysis based on the in-plane theorem is considered to remain for the moment an important verification tool when evaluating the performance of structures consisting of beam/column members. In such cases, appropriate evaluation and judgment of interactions between flexural shear and torsion is required and such results should be reflected in the design and verification process.

Acknowledgements

This research was supported in part by Grand-in-Aid for Scientific Research (B) No. 16360224 (Principal Investigator: K. Kawashima) from the Ministry of Education, Culture, Sports, Science and Technology, Japan.

References

An, X., Maekawa, K. and Okamura, K. (1998). "Numerical simulation of size effect in shear strength of RC beams." *Concrete Library International of JSCE*, No.31, 323-346.

Collins, M. P. and Vecchio, F. (1982). "The response of reinforced concrete to in-plane shear and normal stresses." *University of Toronto*.

Collins, M. P. and Mitchell, D. (1991). "Prestressed concrete structures." *Prentice Hall Inc*.

Dhakal, R. P. and Maekawa, K. (2002a). "Modeling for postyield buckling of reinforcement." *Journal of Structural Engineering*, ASCE, 128 (9), 1139-1147.

Dhakal, R. P. and Maekawa, K. (2002b). "Reinforcement stability and fracture of cover concrete in reinforcement concrete members." *Journal of Structural Engineering*, ASCE, 128 (10), 1253-1262.

El-Kashif, K. F. and Maekawa, K. (2004a). "Time-dependent nonlinearity of compression softening in concrete." *Journal of Advanced Concrete Technology*, 2 (2), 233-248.

El-Kashif, K. F. and Maekawa, K. (2004b). "Time-dependent post-peak softening of RC members in flexure." *Journal of Advanced Concrete Technology*, 2 (3), 301-315.

Hsu, H. L. and Wang, C. L. (2000). "Flexural-torsional behavior of steel reinforced concrete members subjected to repeated loading." *Earthquake Engineering and Structural Dynamics*, Vol. 29, 667-682.

Japan Road Association (1996). "*Specifications for Highway Bridges – Part V Seismic Design*." Tokyo, *Maruzen*.

Japan Society of Civil Engineers (2002). "*Standard Specifications for Concrete Structures 2002 - structural performance verification -*." Tokyo.

Kosaka, H., Ogasawara, M., Sasaki, K., Tsuno, K. Watanabe, E., Tanaka, K. and Sakata, E. (1997). "Experimental study of seismic behavior of RC piers with various ties." *Proc. of JCI symposium on seismic retrofitting techniques for concrete structures*, 87-96. (in Japanese)

Kawashima, K. (2006). "Specimen TP90~99." <http://seismic.cv.titech.ac.jp/ja/titdata/titdata.html>

Maekawa, K., Pimanmas, A. and Okamura, H. (2003). "*Nonlinear Mechanics of Reinforced Concrete*." *SPON Press*.

Maekawa, K., Toongoenthong, K., Gebreyouhannes, E. and Kishi, T. (2006). "Direct path-integral scheme for fatigue simulation of reinforced concrete in shear." *Journal of Advanced Concrete Technology*, 4 (1), 159-177.

Maekawa, K. and El-Kashif K. F. (2004). "Cyclic cumulative damaging of reinforced concrete in post-peak regions." *Journal of Advanced Concrete Technology*, 2 (2), 257-271.

Matsuzaki, H., Mashiko, N., Ichikawa, H. and Tsuchiya, S. (2002). "Residual displacement of seismic resistant reinforced concrete piers subjected to coupled eccentric axial force and torsion." *fib 2002 Osaka Congress*, Disk B Session 6, 287-296.

Nagata, S., Kawashima, K. and Watanabe, G. (2004). "Effect of P-Δ action of actuators in a hybrid loading test." *13th World Conference on Earthquake Engineering*, Vancouver, Canada, Paper No. 881.

Nagata, S., Watanabe, G. and Kawashima, K. (2005). "Effect of P-Δ action of actuators in a hybrid loading test." *Journal of Structural Mechanics and Earthquake Engineering*, No. 801, I-73, JSCE, 197-212. (in Japanese)

Nagataki, S., Okamoto, T. and Lee, S. H., (1988). "A study on mechanism of torsional resistance of reinforced concrete members." *Concrete Library International of JSCE*, No. 12, 75-95.

Otsuka, H., Takeshita, E. and Urakawa, Y. (2005). "Seismic performance and correlation characteristics of reinforced concrete columns subjected to torsional moment, bending moment/shear force and axial force." *Journal of Structural Mechanics and Earthquake Engineering*, No. 801, I-73, JSCE, 123-139.

Okamura, H. and Maekawa, K. (1991). "*Nonlinear Analysis and Constitutive Models of Reinforced Concrete*." Tokyo, *Gihodo-Press*.

Schenk, O. and Gartner, K. (2004). "Solving unsymmetric sparse systems of linear equations with PARDISO." *Future Generation Computer Systems*, 20(3), 475-487.

Tirasit, P., Kawashima, K. and Watanabe, G. (2005). "An experimental study on the performance of RC columns subjected to cyclic flexural-torsional loading." *Proceedings of 2nd International Conference on Urban Earthquake Engineering*, 357-364, Tokyo, Japan.

Tirasit, P. and Kawashima, K. (2006). "Combined cyclic flexural-torsional loading test of RC columns." *Journal of Structural Engineering*, 52A, JSCE, 437-443.

Tirasit, P. and Kawashima, K. (2007). "Seismic performance of square reinforced concrete columns under combined cyclic flexural and torsional loadings." *Journal of Earthquake Engineering* (accepted for publication).

Tsuchiya, S., Tsuno, K. and Maekawa, K. (2002). "Three-dimensional FE solid response analysis of RC columns subjected to a combination of permanent eccentric axial force and reversed cyclic torsion and bending/shear." *Concrete Library International of JSCE*, No.39, 237-252.

Yukawa, Y., Ogata, T., Suda, K. and Saito, H. (1999). "Seismic performance of reinforced concrete high pier with hollow section." *Concrete Library International of JSCE*, No.34.